Carbohydrate Polymers 94 (2013) 364–371

Contents lists available at SciVerse ScienceDirect

Carbohydrate Polymers

journal homepage: www.elsevier.com/locate/carbpol

Antimicrobial electrospun membranes of chitosan/poly(ethylene oxide) incorporating poly(hexamethylene biguanide) hydrochloride

M. Dilamian [a], M. Montazer [b,*], J. Masoumi [c]

[a] Department of Textile Engineering, Islamic Azad University South Tehran Branch, Abozar Blvd., Ahang 1777613651, Tehran, Iran
[b] Department of Textile Engineering, Amirkabir University of Technology, Tehran, Iran
[c] Nanomedicine and Tissue Engineering Research Center, Shahid Beheshti University (M.C.), Taleghani Hospital, Parvaneh St., Velenjak, 1985717443 Tehran, Iran

ARTICLE INFO

Article history:
Received 16 August 2012
Received in revised form 19 January 2013
Accepted 21 January 2013
Available online 28 January 2013

Keywords:
Electrospinning
Chitosan
Nanofiber
Poly(hexamethylene biguanide) hydrochloride (PHMB)
Antimicrobial activity

ABSTRACT

Here, antimicrobial nanofibrous membranes were produced by electrospinning of chitosan/poly(ethylene oxide) (PEO) solution in the presence of poly(hexamethylene biguanide) hydrochloride (PHMB). The influence of PHMB on the electrospinnability and antimicrobial properties of chitosan/PEO nanofibers were studied. Further, viscosity of the solutions as well as morphology of the nanofibrous structures were investigated. Results revealed that incorporation of PHMB in chitosan/PEO solutions led to decrease in the zero-shear rate viscosity up to 20%. Moreover, increasing PHMB from 0.5 mM to 1 mM led to formation of thinner fibers with diameters ranging from 240 nm to 60 nm, respectively. Fourier transform infrared (FT-IR) spectrums indicated the functional groups of chitosan, PEO and PHMB in nanofibrous structure. Differential scanning calorimetry (DSC) thermograms indicated interaction of PHMB with PEO and chitosan through alteration in the thermal behavior of the nanofibers. Inhibition of the bacteria growth for both *Escherichia coli* and *Staphylococcus aureus* were achieved on the PHMB loaded nanofibers. Also, a burst release of PHMB from mats has been observed in the first hour. These findings suggest that there is a great potential in fabrication of biomaterials with incorporation of PHMB using electrospinning.

1. Introduction

Nanofibers are of tremendous interests for a variety of applications due to their useful properties such as high specific surface area and high porosity with small pore size (Huang, Zhang, Kotaki, & Ramakrishna, 2003; Jayaraman, Kotaki, Zhang, Mo, & Ramakrishna, 2004). Many researchers have been focused on the biomedical applications of fibrous and porous structures, such as drug delivery, wound healing, medical prostheses, pharmaceutical composition tissue engineering scaffolds (Sill & Von recum, 2008). Several natural polymers such as gelatin (Zhang, Huang, Xu, Lim, & Ramakrishna, 2004), collagen (Huang, Nagapudi, Apkarian, & Chaikof, 2001), hyaluronic acid (Um, Fang, Hsiao, Okamoto, & Chu, 2004), chitosan (Bhattarai, Edmondson, Veiseh, Matsen, & Zhang, 2005), and wide variety of biodegradable synthetic polymers such as poly(lactic-*co*-glycolide) (PLGA) (Inanç, Arslan, Seker, Elçin, & Elçin, 2009), poly(lactic acid) (PLA) (Tsuji et al., 2006), and poly(ε-caprolactone) (Shalumon et al., 2010) have been successfully electrospun into ultrathin fibers. Nanofibers containing chitin or chitosan yield specific applications in areas such drug delivery (Bhattarai et al., 2005; Ma et al., 2011), tissue engineering and wound healing (Muzzarelli, 2009; Subramanian, Vu, Larsen, & Lin, 2005).

Chitosan, isolated from chitin, is the linear and partly acetylated (1-4)-2-amino-2-deoxy-β-D-glucan (Muzzarelli, 1977, 2012), particularly well known as a functional aid for the ordered regeneration of human tissues (Muzzarelli, 2009). Gradual depolymerization of chitosan leads to release N-acetyl-β-D-glucosamine initiated fibroblast proliferation. This helps collagen deposition and increases level of natural hyaluronic acid synthesis at the wound site. Furthermore, this assists faster wound healing and scar prevention (Ravi Kumar, Muzzarelli, Muzzarelli, Sashiwa, & Domb, 2004; Zhang, Su, Ramakrishna, & Lim, 2008; Zhang, Venugopal, et al., 2008).

Recently, many attempts have been made to produce composite chitosan nanofibrous by blending chitosan with other synthetic biodegradable polymers such as poly(ethylene oxide) (PEO) (Pakravan, Heuzey, & Ajjia, 2011; Ziani et al., 2011) and poly(vinyl alcohol) (PVA) (Ignatova, Starbova, Markova, Manolava, & Rashkov, 2006). In these blends, the fiber forming ability of the co-spinning agent is utilized to facilitate polymer entanglement and generation of a polymer jet (Kriegel, Kit, McClements,

* Corresponding author at: Textile Department, Center of Excellence in Textile, Amirkabir University of Technology, Hafez Avenue, Tehran, Iran.
Tel.: +98 2164542657; fax: +98 2166400245.
E-mail address: tex5mm@aut.ac.ir (M. Montazer).

0144-8617/$ – see front matter © 2013 Elsevier Ltd. All rights reserved.
http://dx.doi.org/10.1016/j.carbpol.2013.01.059

& Weiss, 2009). Electrospinning of chitosan in the presence of poly(ethylene oxide) (PEO), a well-suited fiber-forming polymer, have been widely documented (Bhattarai et al., 2005; Klossner, Hailey, Queen, Coughlin, & Krause, 2008; Kriegel et al., 2009; Ma et al., 2011; Subramanian et al., 2005; Zhang, Su, et al., 2008; Zhang, Venugopal, et al., 2008; Ziani et al., 2011).

Poly(hexamethylene biguanide) hydrochloride (PHMB) is a broad-spectrum antiseptic with excellent tolerance and a low-risk profile (Kaehn, 2010). The aim of therapy using PHMB is to reduce the pathogen burden in a critically colonized or infected acute or chronic wound (Eberlein & Assadian, 2010). Mechanism of antibacterial action of PHMB on a bacterial cytoplasmic membrane has confirmed the adhesion of PHMB to cytoplasmic membranes of bacterial cells, causing them to leak potassium ions and other components within the cytoplasmic fluid resulting in cell death (Gilbert & Moore, 2005).

Due to the high hydration enthalpy of PHMB, hydrophilic-hydrophobic segments of the polymer points in a particular way that form micelle similar to a typical surfactant micelle (De Paula, Netto, & Mattoso, 2011). Incorporation of micelles into nanofibers could modulate the molecular structure and interactions of polymer molecules and further spinnability of the solutions and thus influencing fiber morphology. Ziani et al. (2011) studied the use of Tween 20 and Kriegel et al. (2009) evaluated the effect of anionic sodium dodecyl sulfate (SDS), nonionic polyoxyethylene glycol lauryl ether (Brij 35), and cationic dodecyl trimethyl ammonium bromide (DTAB) on the electrospinning of the cationic chitosan. They reported that the addition of cationic surfactant to polymer solutions increases the positive charge density on the surface of fibers and enhances the whipping instability. The stretch of the jet at higher speed resulted in prevention of beaded fibers and formation of smooth fibers with smaller diameters (Lin, Wang, Wang, & Wang, 2004).

The main objective of this study was to improve antibacterial properties of electrospun chitosan/PEO nanofibers by incorporation of PHMB. The PHMB as antimicrobial agent was mostly chosen for its effectiveness against variety of microorganisms. The influence of PHMB on the viscosity and the spinnability of the solutions and thus the size and morphology of the composite nanofibers were evaluated. The presence of polymer-polymer and surfactant-polymer interactions in compositions of fibers was examined by DSC, and FTIR. The release of PHMB from the composite nanofibrous structures was determined and the antibacterial performance of the samples evaluated using two bacteria including one Gram-positive and one Gram-negative bacteria.

2. Experimental

2.1. Materials

Low molecular weight chitosan with degree of deacetylation (DD) of 75–85% and molecular weight of 120 kDa was prepared from Fluka (Switzerland). Poly(ethylene oxide) (PEO) with a molecular weight of 900 kDa was purchased from Aldrich, USA. Poly (hexamethylene biguanide) hydrochloride (PHMB) was kindly provided by Lonza Co. (Switzerland). Acetic acid was supplied from Merck Co. (Germany). The Gram-positive bacteria *Staphylococcus aureus* and Gram-negative *bacteria Escherichia coli* were used.

2.2. Solutions preparation

A 2.5 wt% chitosan/PEO solution with a mass ratio of 75:25 were prepared by dispersion of chitosan or PEO in 90% acetic acid at room temperature and stirred for 24 h to ensure complete dissolution of the polymers. Solutions containing PHMB below its critical micellar concentration were obtained by dissolving 0.5 mM and 1 mM PHMB in aqueous acetic acid followed by addition and dissolution of chitosan and PEO. All solutions were then used immediately for electrospinning.

2.3. Rheological measurements

The rheological properties of the solutions were characterized at 25 °C using an Anton Paar rheometer (MCR 301) consisted of double concentric cylinder geometry for high viscous solutions and a Ubbelohde capillary viscometer for lower viscous solution. The apparent viscosity of the solutions was determined at 100 s^{-1} from the constant rate curves. The results were fitted to the Ostwald de Waele model, as the most used rheological model, and applied for biopolymer rheo-analysis (Eq. (1)):

$$\tau = k\dot{\gamma}^n \text{ or } \eta_a = k\dot{\gamma}^{n-1} \quad (1)$$

where τ [Pa] is the shear stress, k [Pa s] is consistency coefficient, $\dot{\gamma}$ [s^{-1}] is shear rate, η_a [Pa s] and n are flow behavior index. The flow behavior index (n) is an indicator of whether the solution has a tendency to behave like a shear thinning, shear thickening or Newtonian liquid while the consistency coefficient is an indirect measure of apparent viscosity.

2.4. Electrospinning

Each solution was loaded in a 5 mL syringe with a metal capillary attached. The electrospinning was carried out at 8 kV and 25 °C. The syringe pump delivered polymer solution at a controlled flow rate of 0.3 mL/min. A counter electrode was located at about 13 cm apart from the capillary tip.

2.5. Cross-linking

The electrospun fibrous mats were placed in a dessicator containing 5 mL glutaraldehyde (GA) liquid. The GA liquid vaporized at room temperature (23 °C) and allowed to cross-link the fibers after 2 h.

2.6. Morphology of electrospun nanofibers

The surface morphologies of the electrospun nanofibers were investigated by a scanning electron microscope (SEM; Philips XL30). Nanofiber samples deposited directly onto aluminum foil cut and mounted on aluminum stubs. They were then sputter with gold in a Bal-Tec SCDOOS sputtered coater for 60 s. In order to determine average fiber diameters and their distributions for each electrospun mat, 50 fibers were randomly selected from each SEM images using image analysis software Image-J (National Institutes of Health (NIH)).

2.7. Fourier transform infrared spectroscopy

The ATR-FTIR spectra were recorded at room temperature on a Bruker Tensor 27 spectrometer (Bruker, Karlsruhe). All spectra were taken in the spectral range of 4000–500 cm^{-1} with a 4.0 cm^{-1} resolution. Opus software version 5.5 (Bruker, Karlsruhe) was used to operate the FTIR spectrometer and collect all the data. Measurements were performed on chitosan powder, as-spun PEO, chitosan/PEO and chitosan/PEO/PHMB blend nanofibrous mats.

2.8. Differential scanning calorimetry

Calorimetric measurements of electrospun fibers were carried out using a differential scanning calorimeter (Model Scinco (TGA/DSC) STA N-1500). Weighed samples (approximately 5 mg)

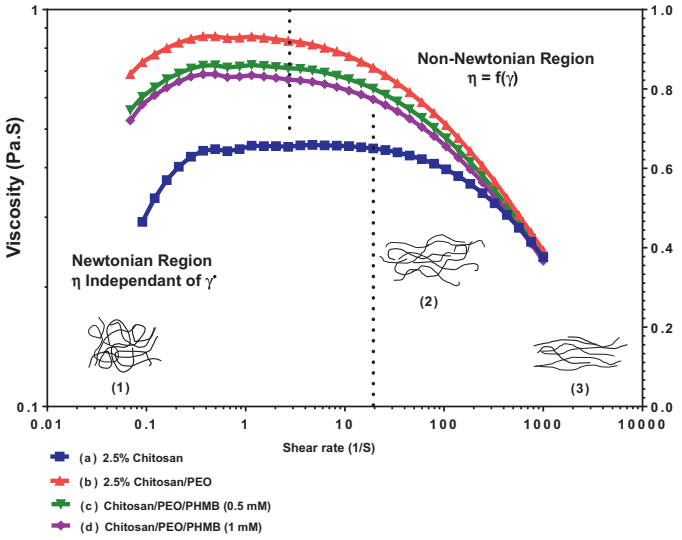

Fig. 1. Shear viscosity as a function of shear rate and pseudoplastic behavior of polymer solutions of chitosan, chitosan/PEO and chitosan/PEO/PHMB in 90% acetic acid solution (polymer concentration = 2.5 wt%). Polymer chains are entangled in Newtonian region (1), and de-entangled with the increase in shear rate (2 and 3).

were sealed in aluminum cups and heated from 25 to 250 °C with a heating rate of 10 °C min^{-1}.

2.9. PHMB release from chitosan-PEO fiber mats

The release characterostic of PHMB from electrospun nanofibers was measured by immersion of nanofibers (3 mg) in 10 mL of distilled water in centrifuge tubes which were kept in a shaking incubator with a shaking speed of 30 rpm at 37 °C. At specific time interval, 2.0 mL of solution was withdrawn and equal amount of the fresh distilled water was replaced. The absorption of PHMB was determined by a UV–VIS Spectrophotometer (Cecil CE 7500 (Elegant Technology)) at the maximal absorption peak with the wavelength of 213 nm. A linear calibration curve ($\gamma^2 = 0.9975$) was obtained between the absorption strength and PHMB concentration range of 0–0.024 mg/mL.

2.10. Antibacterial activity test

The antibacterial activity test against *Staphylococcus aureus* (*S. aureus*) ATCC 25923 and *Escherichia coli* (*E. coli*) ATCC 25922 were carried out using agar disk diffusion method. The samples were cut to small circular pieces (0.8 mL diameter, 0.5 mL thickness). The control sample was prepared by preparation chitosan nanofibers without PHMB. All samples were heated to remove acid content and sterilized under ultraviolate for overnight. The plates were filled with Muller-Hinton agar medium. A transferring loop of bacteria was taken and dispersed on the surface of slope medium evenly. After the plate was inoculated, the samples were placed on it and they were placed in the incubator at 36 ± 1 °C for 24 h.

3. Results and discussion

3.1. Rheological behavior

The viscosity of the polymer solutions is characteristic of intermolecular interactions between polymer chains that strongly affects the spinnability of the solutions and morphology of as-spun fibers (Bhattarai et al., 2005; Huang et al., 2003). Thus, the rheological properties of polymer solutions as a function of shear rate were measured for different solutions. The results in Fig. 1 indicated that the zero-shear viscosity of 2.5% chitosan was 0.43 Pa s while, a 2.5 wt% composite solution of chitosan/PEO with 75:25 ratio showed a higher viscosity (0.73 Pa s) than both of its precursor solutions. This is possibly due to the strong interactions between chitosan and large expanded PEO chains which make sufficient entanglement and facilitate electrospinning (Pakravan et al., 2011; Ziani et al., 2011). The addition of PHMB to chitosan solution with PEO slightly reduced the viscosity to 0.65 Pa s. However, increasing PHMB content to 1 mM, led to reduction in the zero shear viscosity by 10% (0.58 Pa s). Overall, all applied PHMB contents were lowered the critical micelle concentration (CMC).

The flow curves of each polymer solution and their mixture (shear stress, τ, versus shear rate, $\dot{\gamma}$) are well fitted to the Ostwald de Waele model (Eq. (1)) and the values for the consistency index (K), flow behavior index (n) are listed in Table 1. At low shear rates, the solutions are close to Newtonian model while at higher shear rates, the polymer chains orient and align with the flow direction leads to lower viscosity (Fig. 1). The flow behavior index (n) for all polymer solutions are smaller than 1 suggesting a pseudo plastic behavior. All polymer solution shows n value around 0.7 except for chitosan solution which present a higher value ($n = 0.8$), representing less pseudo plasticity. This could be due to the strong intramolecular hydrogen bonding between chitosan chains which resist with disentanglements at higher shear rates.

The consistency coefficient of all solutions showed similar trends as the apparent viscosity. K, significantly increased when the PEO was added to the neat chitosan solution and with increasing concentrations of PHMB (0.5 and 1 mM), K values decreased from 1.90 to 1.72, respectively. This is directly related to the extent of polymer molecule chain arrangement as a critical factor in fiber formation. If polymers are not or insufficiently entangled, beads or droplets instead of fibers are typically deposited on the collector plate (Kriegel et al., 2009).

The critical overlap concentration (C^*) is the crossover concentration at which the entanglement of polymer chains start as one of the most important characteristic of a polymer solution and a critical parameter for electrospinning. The critical overlap concentration was determined from intrinsic viscosity as:

$$C^* \sim [\eta]^{-1}$$

Table 1
Power law flow behavior index (n), consistency coefficient (K) and apparent viscosity at a shear rate of 100 s^{-1} for chitosan, PEO, PHMB and their blends in 90% acetic acid solutions.

Solutions in 90% acetic acid	Power law flow behavior index K	Power law consistency coefficient n	Apparent viscosity $\eta_{a,100}$ (Pa s)
2.5% Chitosan	1.20 ± 0.05	0.80 ± 0.01	0.45 ± 0.003
Chitosan/PEO	2.17 ± 0.08	0.70 ± 0.01	0.53 ± 0.002
Chitosan/PEO/PHMB (0.5 mM)	1.90 ± 0.07	0.70 ± 0.01	0.50 ± 0.002
Chitosan/PEO/PHMB (1 mM)	1.72 ± 0.06	0.71 ± 0.01	0.45 ± 0.001

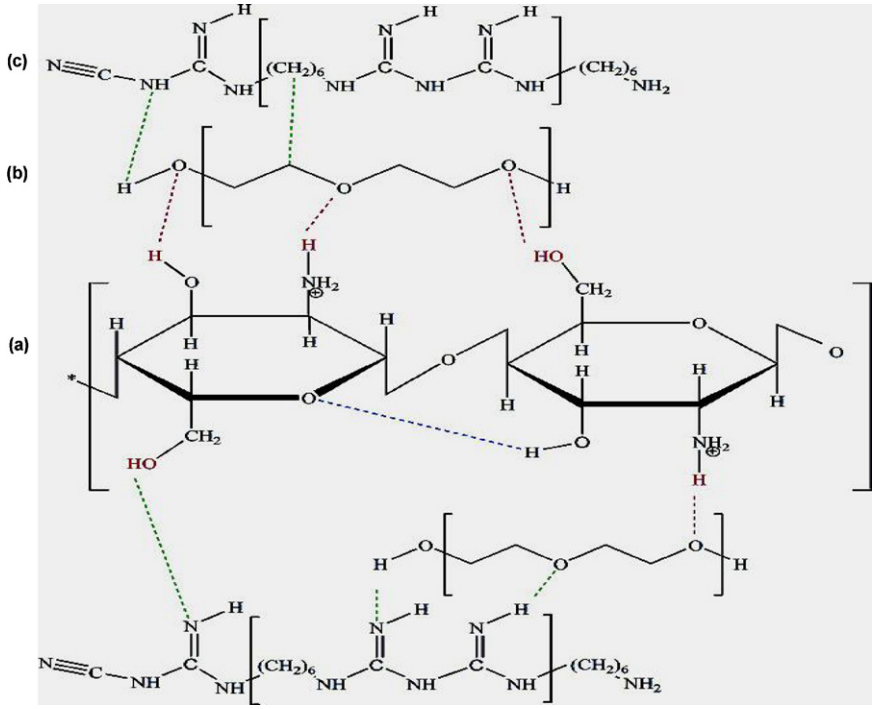

Fig. 2. Chemical structures and polymer-polymer interactions of (a) chitosan, (b) PEO and (c) PHMB.

Polymer concentration had to be increased to $C{\sim}6C^*$ for uniform fiber formation to occur with polymers of a narrow molecular weight distribution (MWD) and even higher concentrations were required in case of broad MWD (Kriegel et al., 2009). In this work, C^* was determined to be 0.105 g/dL which was much lower than the concentration used for electrospinning. Since, chitosan and PHMB both yielding a highly cationic polyelectrolyte at low pH, there were an increased electrostatic repulsion between their ammonium ions, $-NH_3^+$. Nevertheless, PHMB still may bind to the PEO through its hydrophobic and hydrophilic segments. If binding occurred electrostatic repulsive forces may increase and interactions between polymers molecules may decrease, resulting in decreased entanglement and lower viscosity. Thus, finer fibers were obtained by addition of PHMB (Fig. 2).

3.2. Morphology of nanofibers

The morphology of electrospun nanofibers is demonstrated in Fig. 3. Pure chitosan did not form fibers and only beads or drops in the range of 328 nm were deposited. It has been hypothesized that the repulsive forces between ionic groups within polymer backbone increased due to the application of a high electric field during electrospinning restricted formation of continuous fibers and produced particles (Pakravan et al., 2011; Ziani et al., 2011). Addition of PEO to the chitosan solution, disrupt the self-association of chitosan chains by formation of additional hydrogen bondings between its hydroxyl groups and water molecules. This led to a reduction in the repulsive forces between polycationic groups improved chain entanglement and induce production of fibers (Bhattarai et al., 2005). As it is clear in Fig. 3(a) defect free chitosan/PEO nanofiber with the average diameter of 272 nm lower the neat PEO nanofiber were successfully produced.

Fig. 3b and c shows SEM images of nanofibers with 0.5 mM and 1 mM PHMB at the chitosan/PEO ratio of 75:25. All polymer dispersions supplemented with PHMB were capable of forming nanofibers. The average size of electrospun structure containing 0.5 mM and 1 mM PHMB decreased to 183 nm and 153 nm, respectively. By adding PHMB, the conductivity of the solution increased that is required a lower electric field. Moreover, higher conductivity may result in higher charge densities being present at the surface of fibers, which may lead to higher forces, stretching the polymer jet and thus promote thinner jets. This yielded fibers with a smaller diameter (Kriegel et al., 2009). However, addition of PHMB above the critical micellar concentration (CMC) (De Paula et al., 2011) led to insoluble complexes that rapidly caused phase separation from solution. Thus, nanofiber formation was impossible with PHMB content above CMC.

3.3. DSC results

The DSC thermograms of chitosan, PEO raw materials as well as chitosan/PEO and their blends with PHMB are shown in Fig. 4. A sharp peak was observed at 75 °C for pure PEO (Fig. 4(b)) related to its melting. The characteristic endothermic peaks of chitosan was observed at 80 °C (Fig. 4(a)) termed as dehydration temperature (T_D) (Neto et al., 2005), due to water bound to the amine groups of chitosan. At low water content, the water molecules can be released below 100 °C (Min et al., 2004). The endothermic peak of chitosan/PEO (at 68.74 °C) showed a reduction by almost 6.26 °C and 11.26 °C comparing with the pure PEO and chitosan, respectively (Fig 4(c)). This shift to the lower temperature reflected a favorable interaction between crystalline PEO and amorphous chitosan chains by formation of strong intermolecular hydrogen bonds between the ether groups of PEO and the amino/hydroxyl groups of chitosan (Chen, Mo, He, & Wang, 2008). PHMB has an amorphous nature with glass transition temperature in the range of 60–80 °C (De Paula et al., 2011). Addition of PHMB to chitosan/PEO blend slightly shifted the endothermic peak to 62.5 °C (Fig. 4(d)). At low pH chitosan and PHMB both behave as a cationic polyelectrolyte and repulsive interactions between ammonium ions predominant. Hence, this shift may assigned to the exothermic effect of interpolymer interaction between the methylene and amine groups of biguanide and ethylene and ether groups of PEO, respectively. The

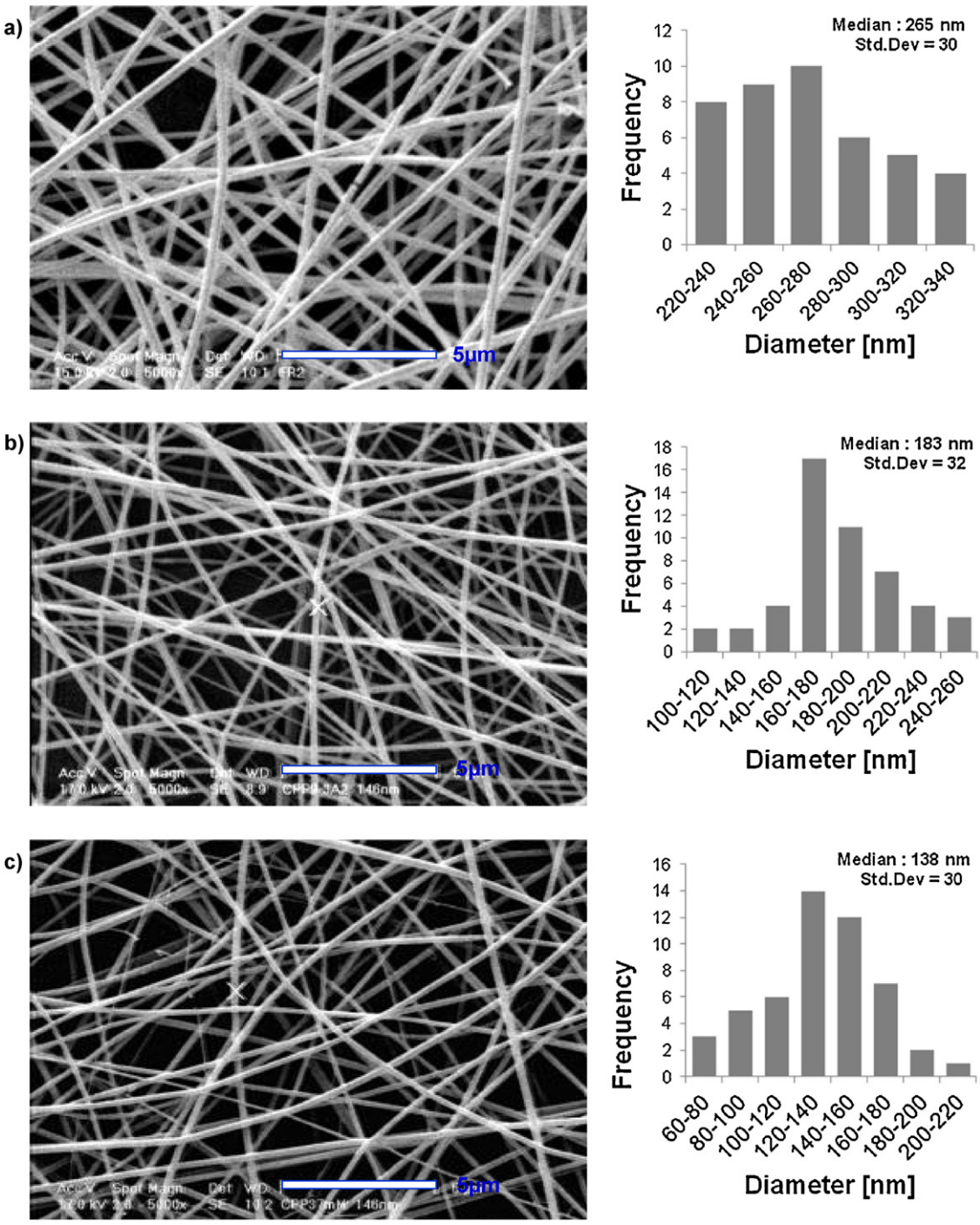

Fig. 3. SEM micrograph of electrospun structures prepared from different solutions of (a) 2.5 wt% chitosan/PEO (3:1, w/w), chitosan/PEO (3:1, w/w) containing: (b) 0.5 mM and, (c) 1 mM PHMB.

results are in a good agreement with the solution viscosity reduction after addition of PHMB (Fig. 2).

3.4. FT-IR spectroscopy

FT-IR spectra of chitosan, PEO, chitosan/PEO and chitosan/PEO/PHMB nanofibers are shown in Fig. 5. The main characteristic bands of pure chitosan (Fig. 5(e)) due to N—H and OH···O stretching vibration and inter molecular hydrogen bonding of chitosan backbone was observed at 3357 cm^{-1} (Rakkapao, Vao-soongnern, Masubuchi, & Watanabe, 2011). The feature peaks of amide I and amid II (N—H bending vibration) are seen at 1610 cm^{-1} and 1591 cm^{-1}, respectively. The peak at 2870 cm^{-1} was attributed to the CH_2 stretching, and the one at 1099 cm^{-1} was due to the anti-symmetric stretching of C—O—C bridge. A typical absorption bands was observed at 2884 cm^{-1} for the PEO as spun nanofiber (Fig. 5(a)) assigned to CH_2 stretching vibration, which can overlapped with the one in chitosan (Rakkapao et al., 2011). Other characteristic peaks are seen at 1099 cm^{-1} and 962 cm^{-1} due to stretching vibration of ether (C—O—C) group. By adding PEO, the vibration bands of amino (1591 cm^{-1}) and hydroxyl/amine (3357 cm^{-1}) of chitosan were shifted to 1560 cm^{-1} and 3364 cm^{-1},

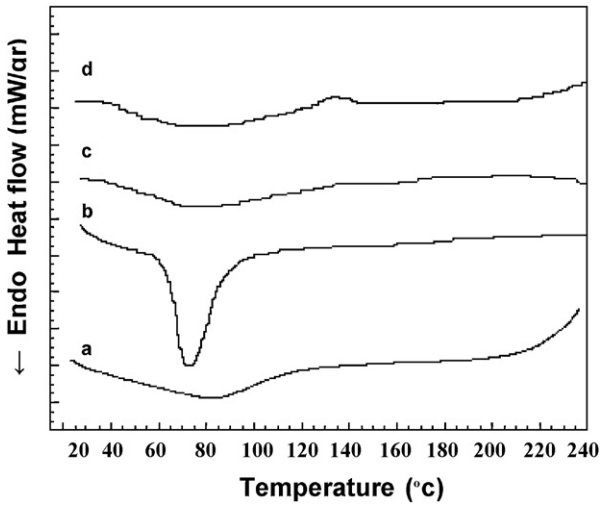

Fig. 4. DSC thermogram curves of (a) chitosan powder, (b) electrospun PEO nanofibers, (c) chitosan/PEO nanofibers and (d) chitosan/PEO nanofibers containing 1 mM PHMB.

respectively. While, the absorbance intensity of these peaks decreased, the absorbance intensity of CH_2 groups at 2870 cm^{-1} increased (Fig. 5(b)) (Rakkapao et al., 2011). This structure changes may be due to considerable decrease in intermolecular hydrogen bonding of chitosan molecules and formation of new hydrogen bonds between oxygen of polyether and hydrogen of amine group in PEO and chitosan, respectively (Chen et al., 2008). The characteristic absorption peaks for PHMB are observed at (Fig. 5(c)) 3300 cm^{-1}, 1650 cm^{-1} and about 1587 cm^{-1} attributed to N—H stretching vibration, C=N stretching and bend vibration of NH_2^+, respectively. Adding PHMB to chitosan/PEO solution, the characteristic peaks for chitosan and PEO remained unchanged except for their intensity. The absorbance intensity of NH_2 groups at 3361 cm^{-1} (N—H stretching) and C=N imine groups at about 1650 cm^{-1} increased, if the CH_2 at 1343 cm^{-1} is taken as the datum peak. Moreover, the amide II at 1560 cm^{-1} slightly shifted to 1587 cm^{-1}. This shift may be caused by repulsive forces of cationic PHMB and chitosan besides formation of new hydrogen bonds between hydrogen and oxygen from PHMB and PEO respectively. The FTIR spectra of cross-linked chitosan nanofibers with GA, displayed an increase in the absorbance intensity of C=N imine band at 1655 cm^{-1}. This peak proved that GA cross-linked chitosan nanofiber through the Schiff base mechanism (Fig. 5(d)) (Zhang, Jiang, & Chen, 1999).

3.5. PHMB release

The release profile of PHMB from Chitosan/PEO electrospun nanofiber is shown in Fig. 7. An initial burst release of more than 63.62% of PHMB is observed in the first 3 h which followed steadily to 70.21% of PHMB for 4 h. The rate became slower for the next hour until the equilibrium reached at 24 h with 85% PHMB release. The rate of diffusion-controlled drug release depends on three main

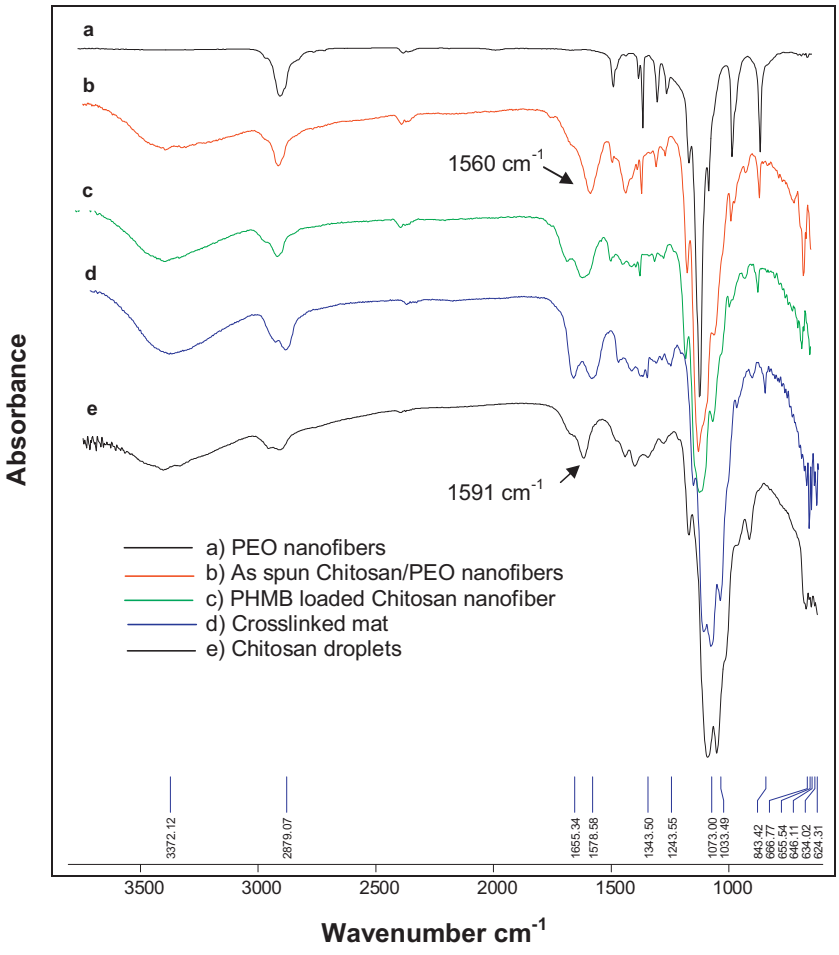

Fig. 5. FT-IR spectra of (a) as spun PEO, blend nanofibrous mats of (b) chitosan/PEO, (c) PHMB loaded chitosan/PEO nanofiber, (d) crosslinked chitosan/PEO with PHMB content and (e) chitosan droplets.

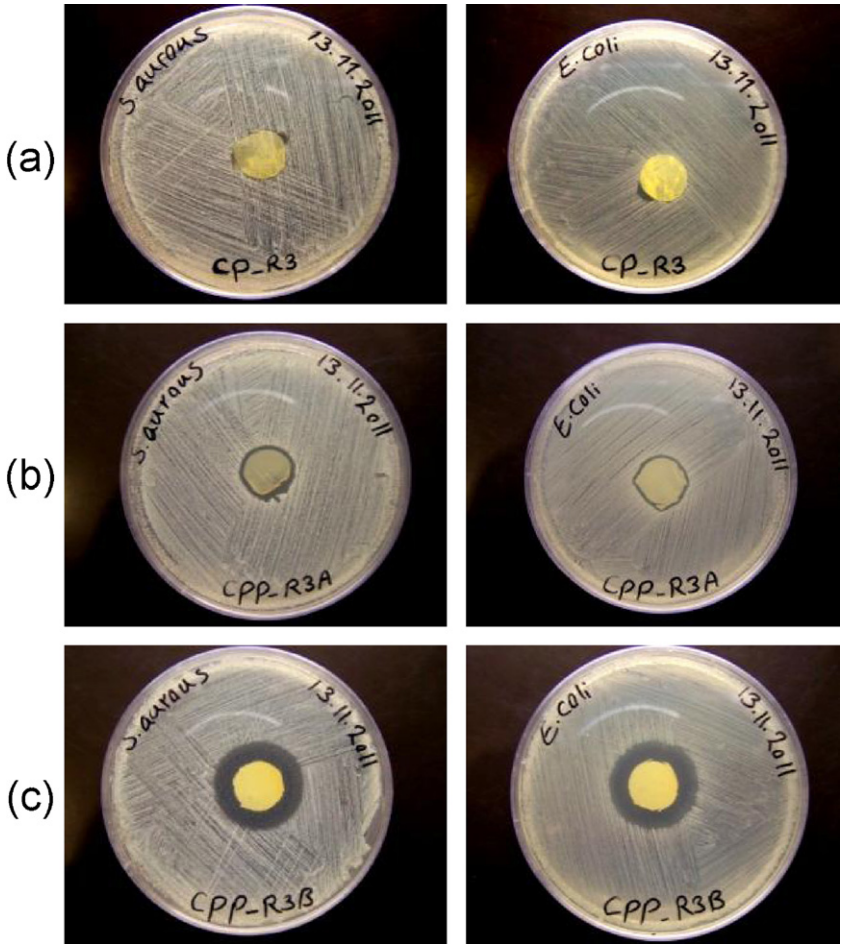

Fig. 6. Bacterial growth inhibition by modified Kirby-Bauer disc method. Scaffold were incubated at 37 °C for 24 h on agar plates cultured with *Staphylococcus aureus* (left panel) and *E. coli* (right panel). chitosan/PEO nanofiber (weight ratio of 75:25) (a) control sample without, (b) 0.5 mM PHMB and (c) with 1 mM PHMB.

factors: (1) dissolvability of the drug in the release medium, (2) ease of the medium to penetrate the polymer and drug matrix and (3) physical attractions or chemical bonds between the polymer and the drug (Liu, Leonas, & Zhao, 2010).

Both Chitosan and PHMB have high positive charge density and the strong repulsive forces among their polymer chains may force PHMB to orient along the surface of the nanofibers and link with PEO polymer through some hydrogen bondings and van der waals forces. The high surface area and porous structure of membrane enable the penetration of water molecule and the diffusion-controlled release of dissolved PHMB to the medium. Moreover, by penetrating of water through chitosan/PEO nanofibers, the fibers swelled due to the good swelling properties of chitosan and PEO polymers. Hence, water content increased within fibers and the diffusion rate of PHMB into the water rapidly increased.

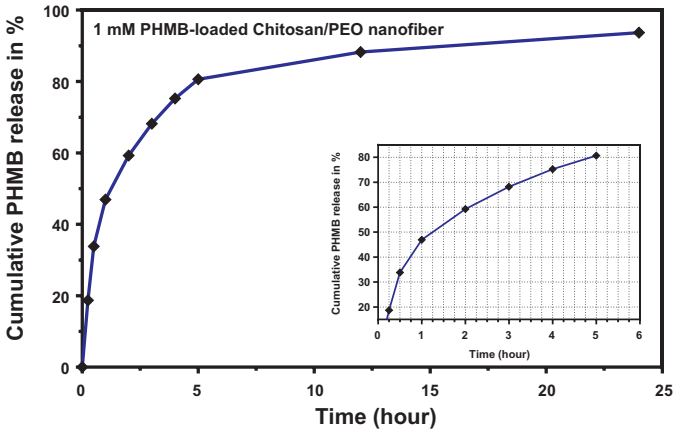

Fig. 7. Release profiles of PHMB from chitosan-PEO nanofiber by immersing 1 mM PHMB- loaded fibers into distilled water at 37 °C.

3.6. Antibacterial activity test

PHMB has been in use as an antiseptic and disinfectant for approximately 60 years with proven effectiveness against a broad number of bacterial and fungal species with rapid and sustained action (Butcher, 2010). It has been shown the greater killing effect with less host toxicity for PHMB than chlorhexidine, povidone-iodine, triclosan, silver and sulfadiazine (Koburger, Hubner, Braun, Siebert, & Kramera, 2010). The antibacterial activity of prepared chitosan/PEO and chitosan/PEO/PHMB composite nanofibers were investigated by disc diffusion method against *E. coli* and *S. aureus*. As the test disk is applied onto the inoculated surface of the test medium the wetted disks absorb water from the agar medium and the release of the antimicrobial is initiated and PHMB migrates through the adjacent agar medium. As a result, a gradually changing gradient of the antibacterial concentration develops in the agar surrounding the disk. No clear zone was observed between the control sample and the bacterial colonies (Fig. 6(a)). Zone of inhibition for the sample contained 0.5 mM PHMB were 13.8 mm and 12 mm for *S. aureus* and *E. coli*, respectively (Fig. 6(b)). By increasing the PHMB content to 1 mM, the growth inhibition zone diameter increased to

22 mm and 21.1 mm for *S. aureus* and *E. coli*, respectively (Fig. 6(c)). Thus, the novel chitosan/PEO/PHMB nanocomposite exhibited an excellent antibacterial activity.

4. Conclusion

Addition of PHMB to chitosan solution indicated a significant influence on the morphology and properties of the prepared nanoweb structures. SEM images showed the smooth nanofibers with the mean diameter of 138 nm obtained with high PHMB content. Compositional analysis suggested PHMB interaction with polar and nonpolar sections of PEO and chitosan, resulted in modified properties of nanofibers. Solution viscosity and SEM images suggested positive influence of PEO chains to produce sufficient entanglement and to enhance the electrospinnability of chitosan nanofiber. Moreover, addition of PHMB decreased interactions between polymer chains reduced the solution viscosity. The release profile revealed burst depletion of 70% PHMB in the first hour for chitosan/PEO nanofibers loaded with 1 mM PHMB. This can be attributed to the accumulation of PHMB on the fiber surface, the small fiber diameter and swelling properties of chitosan and PEO. The porous mats containing PHMB not only provides a barrier to *S. aureus* and *E. coli* but also inhibits the growth of bacteria within the dressing. These findings suggest that there is a great potential in fabrication of biomaterials with incorporation of PHMB using electrospinning.

Acknowledgements

The authors would like to thank Mr. Janmaleki and Mr. Taranejoo at Nanomedicine and Tissue Engineering Research Center, at Shahid Beheshti University for their experimental assistance.

References

Bhattarai, N., Edmondson, D., Veiseh, O., Matsen, F. A., & Zhang, M. (2005). Electrospun chitosan-based nanofibers and their cellular compatibility. *Biomaterials*, *26*, 6176–6184.

Butcher, M. (2010). Bacterial management: in modern wound. *Wound Essentials*, *5*, 126–199.

Chen, Z., Mo, X., He, C., & Wang, H. (2008). Intermolecular interactions in electrospun collagen–chitosan complex nanofibers. *Carbohydrate Polymers*, *72*, 410–418.

De Paula, G. F., Netto, G. I., & Mattoso, L. H. C. (2011). Physical and chemical characterization of poly(hexamethylene biguanide) hydrochlorid. *Polymers*, *3*, 928–994.

Eberlein, T., & Assadian, O. (2010). Clinical use of polihexanide on acute and chronic wounds for antisepsis and decontamination. *Skin Pharmacology and Physiology*, *23*, 45–51.

Gilbert, P., & Moore, L. E. (2005). Cationic antiseptics: diversity of action under a common epithet. *Applied Microbiology*, *99*, 703–715.

Huang, L., Nagapudi, K., Apkarian, R. P., & Chaikof, E. L. (2001). Engineered collagen-PEO nanofibers and fabrics. *Biomaterials Science: Polymer Edition*, *129*, 79–93.

Huang, Z. M., Zhang, Y. Z., Kotaki, M., & Ramakrishna, S. (2003). A review on polymer nanofibers by electro-spinning applications in nanocomposites. *Composites Science and Technology*, *63*, 2223–2253.

Ignatova, M., Starbova, K., Markova, N., Manolava, N., & Rashkov, I. (2006). Electrospun nanofibre mats with antibacterial properties from quaternised chitosan and poly (vinyl alcohol). *Carbohydrate Research*, *341*, 2098–2107.

Inanç, B., Arslan, Y., Seker, S., Elçin, A., & Elçin, Y. (2009). Periodontal ligament cellular structures engineered with electrospun poly(DL-lactide-co-glycolide) nanofibrous membrane scaffolds. *Biomedical Materials Research Part A*, *90*, 186–195.

Jayaraman, K., Kotaki, M., Zhang, Y., Mo, X., & Ramakrishna, S. (2004). Recent advances in polymer nanofibers. *Nanoscience and Nanotechnology*, *4*, 52–56.

Kaehn, K. (2010). Polihexanide: a safe and highly effective biocide. *Skin Pharmacology and Physiology*, *23*, 7–16.

Klossner, R., Hailey, A., Queen, H., Coughlin, A., & Krause, W. (2008). Correlation of chitosan's rheological properties and its ability to electrospin. *Biomacromolecules*, *9*, 2947–3295.

Koburger, T., Hubner, N.-O., Braun, M., Siebert, J., & Kramera, A. (2010). Standardized comparison of anriseptic efficacy of triclosan, PVP-iodine, octenidine dihydrochloride, polyhexanide and chlorhexidine digluconate. *Antimicrobial Chemotherapy*, *65*, 1712–1719.

Kriegel, C., Kit, K. M., McClements, D. J., & Weiss, J. (2009). Electrospinning of chitosan-poly(ethylene oxide) blend nanofibers in the presence of micellar surfactant solutions. *Polymer*, *50*, 189–200.

Lin, T., Wang, H., Wang, H., & Wang, X. (2004). Charge effect of cationic surfactants on the elimination of fibre beads in the electrospinning of polystyrene. *Nanotechnology*, *15*, 1375–1381.

Liu, H., Leonas, K., & Zhao, Y. (2010). Antimicrobial properties and release profile of ampicillin from electrospun poly(ε-caprolactone) nanofiber yarns. *Journal of Engineered Fibers and Fabrics*, *5*, 10–19.

Ma, G., Liu, Y., Peng, C., Fang, D., He, B., & Nie, J. (2011). Paclitaxel loaded electrospun porous nanofibers as mat potential application for chemotherapy against prostate cancer. *Carbohydrate Polymers*, *86*, 505–512.

Min, B. M., Won Lee, S., Nam Lim, J., Young, Y., Taek Seung, L., Hyun Kang, P., et al. (2004). Chitin and chitosan nanofibers: electrospinning of chitin and deacetylation of chitin nanofibers. *Polymer*, *45*, 7137–7142.

Muzzarelli, R. A. A. (1977). *Chitin*. Oxford, UK: Pergamon Press.

Muzzarelli, R. A. A. (2009). Chitins and chitosans for the repair of wounded skin, nerve, cartilage and bone. *Carbohydrate Polymers*, *76*, 167–182.

Muzzarelli, R. A. A. (2012). Nanochitins and nanochitosans, paving the way to eco-friendly and energy-saving exploitation of marine resources. In K. Matyjaszewski, & M. Möller (Eds.), *Polymer science: a comprehensive reference* (pp. 153–164). Amsterdam: Elsevier BV.

Neto, C. G. T., Giacometti, J. A., Job, A. E., Ferreira, F. C., Fonseca, J. L. C., & Pereira, M. R. (2005). Thermal analysis of chitosan based networks. *Carbohydrate Polymers*, *62*, 97–103.

Pakravan, M., Heuzey, M., & Ajjia, A. (2011). A fundamental study of chitosan/PEO electrospinning. *Polymer*, *52*, 4813–4824.

Rakkapao, N., Vao-soongnern, V., Masubuchi, Y., & Watanabe, H. (2011). Miscibility of chitosan/poly(ethylene oxide) blends and effect of doping alkali and alkali earth metal ions on chitosan/PEO interaction. *Polymer*, *52*, 2618–2627.

Ravi Kumar, M. N. V., Muzzarelli, R. A. A., Muzzarelli, C., Sashiwa, H., & Domb, A. J. (2004). Chitosan chemistry and pharmaceutical perspectives. *Chemical Reviews*, *104*, 6017–6084.

Shalumon, K. T., Anulekha, K. H., Girish, C. M., Prasanth, R., Nair, S. V., & Jayakumar, R. (2010). Single step electrospinning of chitosan/poly (caprolactone) nanofibers using formic acid/aceton solvent mixture. *Carbohydrate Polymers*, *80*, 413–419.

Sill, T. J., & Von recum, H. A. (2008). Electrospinning: applications in drug delivery and tissue engineering. *Biomaterials*, *29*, 989–2006.

Subramanian, A., Vu, D., Larsen, G. F., & Lin, H. Y. (2005). Preparation and evaluation of the electrospun chitosan/PEO fibers for potential application in cartilage tissue engineering. *Biomaterials Science: Polymer Edition*, *16*, 861–873.

Tsuji, H., Nakano, M., Hashimoto, M., Takashima, K., Katsura, S., & Mizuno, A. (2006). Electrospinning of poly(lactic acid) stereocomplex nanaofibers. *Biomacromolecules*, *7*, 3316–3320.

Um, I., Fang, D., Hsiao, B., Okamoto, A., & Chu, B. (2004). Electrospinning and electroblowing of hyaluronic acid. *Biomacromolecules*, *5*, 1428–1436.

Zhang, Y., Jiang, J., & Chen, Y. (1999). Synthesis and antimicrobial activity of polymeric guanidine and biguanidine salts. *Polymer*, *40*, 6189–6198.

Zhang, Y., Venugopal, J., Turki, A., Ramakrishna, S., Su, B., & Lim, C. (2008). Electrospun biomimetic nanocomposite nanofibers of hydroxyapatite/chitosan for bone tissue engineering. *Biomaterials*, *29*, 4314–4322.

Zhang, Y. Z., Huang, Z. M., Xu, X. J., Lim, C. T., & Ramakrishna, S. (2004). Preparation of core-shell structured PCL-r-Gelatin Bi-component nanofibers by coaxial electrospinning. *Chemistry of Materials*, *16*, 3406–3409.

Zhang, Y. Z., Su, B., Ramakrishna, S., & Lim, C. T. (2008). Chitosan nanofibers from an easily electrospinnable UHMWPEO-doped chitosan solution system. *Biomacromolecules*, *9*, 136–141.

Ziani, K., Henrist, C., Jérôme, C., Aqil, A., Maté, J. I., & Cloots, R. (2011). Effect of nonionic surfactant and acidity on chitosan nanofibers with different molecular weights. *Carbohydrate Polymers*, *83*, 470–476.